Experimental Calcification of HEMA-Based Hydrogels in the Presence of Albumin and a Comparison to the in Vivo Calcification

Zainuddin,[†,‡] David J. T. Hill,[†] Traian V. Chirila,*[,‡,§,||] Andrew K. Whittaker,[§,⊥] and Anne Kemp[¶]

Department of Chemistry, University of Queensland, Santa Lucia, Brisbane, Queensland 4072, Australia, Queensland Eye Institute, University of Queensland, 41 Annerley Road, South Brisbane, Queensland 4101, Australia, Australian Institute for Bioengineering and Nanotechnology, University of Queensland, Santa Lucia, Brisbane, Queensland 4072, Australia, School of Physical and Chemical Sciences, Queensland University of Technology, Brisbane, Queensland 4001, Australia, Centre for Magnetic Resonance, University of Queensland, Santa Lucia, Brisbane, Queensland 4072, Australia, and Centre for Microscopy and Microanalysis, University of Queensland, Santa Lucia, Brisbane, Queensland 4072, Australia

Received January 23, 2006; Revised Manuscript Received March 23, 2006

The precipitation patterns and characteristics of calcium phosphate (CaP) phases deposited on HEMA-based hydrogels upon incubation in simulated body fluid (SBF-2) containing a protein (human serum albumin) have been investigated in relation to the calcification in an organic-free medium (SBF-1) and to that occurring after subcutaneous implantation in rats. In SBF-2, the deposits occurred exclusively as a peripheral layer on the surface of the hydrogels and consisted mainly of "precipitated hydroxyapatite", a species deficient in calcium and hydroxyl ions, similarly to the deposits formed on the implanted hydrogels, where the deposited layer was thicker. In SBF-1, the deposits were mainly of brushite type. There was no evidence that albumin penetrated the interstices of hydrogels. As the X-ray diffraction patterns of the CaP deposits generated in SBF-2 showed a similar nature with those formed on the implanted hydrogel, it was concluded that the calcification in SBF-2 can mimic to a reliable extent the calcification process taking place in a biological environment.

Introduction

The term hydrogels denotes water-swelling polymers, either natural or synthetic. Synthetic hydrogels, especially those based on 2-hydroxyethyl methacrylate (HEMA, henceforth the homopolymer is designated as PHEMA) and other hydrophilic monomers, are widely used as biomaterials, e.g., in the eye health care (contact lenses, ocular implants), in dentistry, in controlled drug release, and tentatively in orthopedic and cardiovascular applications. Like any other polymeric biomaterial, the hydrogels can undergo dystrophic calcification following their contact with, or placement within, living tissues. The biomaterials-associated calcification involves the deposition of calcium phosphate phases similar to hydroxyapatite, henceforth designated as CaP, on the biomaterial itself and/or on the host tissues. Depending on the particular field of application, the calcification of hydrogels during their task life is either pursued or avoided. The ocular applications of hydrogels, both vision-corrective (contact lenses) and vision-restorative (artificial intraocular lenses, artificial corneas), require the use of transparent hydrogels and also the indefinite maintenance of their transparency; therefore, calcification must be prevented. On the contrary, in dental implants or in orthopedic applications aiming at bone substitution or repair, the deposition of hydroxyapatite on biomaterials is beneficial.

Our work has been directed at elucidating the mechanism of spontaneous calcification of transparent hydrogels and at finding means to prevent the process. The spoliation of ocular devices due to calcium-containing deposits on the surface or inside the hydrogels is well documented.[1−6] There is also convincing evidence[7] that HEMA-based hydrogels undergo calcification when placed inside living tissues. Such hydrogels have in fact an inherent propensity to induce the spontaneous precipitation of CaP onto and within the polymer matrix, even in the absence of any biological agent (i.e., in abiogenic conditions), in other words in nothing else but aqueous solutions of calcium ions and phosphate ions. After having discussed a range of potential scenarios for the spontaneous abiogenic calcification of HEMA-based hydrogels,[7] we demonstrated that the enhancement of supersaturation within the polymer network due to local salting-out ionic solute effects and the diffusion gradients can both plausibly contribute to the mechanism,[8,9] and that the abiogenic calcification may be, after all, as complex as that suggested for the biogenic process involving biopolymers as substrates,[10] due to structural and surface energetic factors yet to be elucidated.

Calcification of hydrogels has been so far assessed in vitro almost exclusively in simulated body fluid (SBF) formulations devoid of organic constituents. However, spoliation of PHEMA in a simulated eye's aqueous humor containing amino acids, glucose, urea, and albumin, in the presence of ocular drugs,

* To whom correspondence should be addressed. Fax: 61-7-3010-3390. E-mail: traian.chirila@pbf.org.au.
† Department of Chemistry, University of Queensland.
‡ Queensland Eye Institute.
§ Australian Institute for Bioengineering and Nanotechnology, University of Queensland.
|| Queensland University of Technology.
⊥ Centre for Magnetic Resonance, University of Queensland.
¶ Centre for Microscopy and Analysis, University of Queensland.

10.1021/bm060075g CCC: $33.50
Published on Web 05/06/2006

has been recently reported.[6,11] Although a frequent feature, calcium was not always present in the drug-induced deposits, and the results could not be extrapolated to a real clinical situation due to factors such as drug concentration, instability of the simulated aqueous humor, and absence of the natural inhibitors of mineralization. Generally speaking, calcification of hydrogels in vivo is expected to be different from that assessed in vitro in organic-free SBF solutions. The best we can do to make the assays comparable is to add proteins to the SBF.

Adsorption of proteins on the substrate and/or their presence in the surrounding biological fluid is of great significance for the biomineralization process. A dual and opposite effect of the presence of proteins has been generally demonstrated in a number of studies, as recently reviewed.[12] For instance, a protein can promote nucleation when adsorbed on a solid substrate in the right template arrangement, but the same protein can have an inhibitory effect on the crystal growth when present as a solute in the surrounding medium. This duality may be due to different activities of the proteins in specific stages of the mineralization process. Certain proteins may inhibit nucleation and promote crystal growth, while other proteins may act in a completely opposite way. The contradictory effects reported so far may originate not only from the complexity of the mineralization process but also from the source and quality of the proteins used in experiments and the design of experiments.

Albumin is a ubiquitous protein in the body fluids and is involved in many physiological processes. Albumin is implicated in the transport, distribution, and metabolism of various ligands, including fatty acids, steroids, amino acids, and metals. Its binding affinity for calcium in physiological conditions has been demonstrated,[13−15] and its dual role in the precipitation of calcium phases has been proved in several instances.[12,16−19] As the most abundant plasma protein and as one of the most important noncollagenous proteins to be involved in the formation of hard tissues, albumin is highly suitable as an additional constituent to the SBF formulations in order to make the in vitro and in vivo assays more comparable and to assess whether the role of proteins in vitro is similar to that observed in the in vivo calcification of HEMA-based hydrogels. This is the aim of the present study. PHEMA and three other copolymer hydrogels based on HEMA were subjected to an in vitro calcification experiment, both in organic-free SBF (henceforth, SBF-1) and in SBF containing human serum albumin (henceforth, SBF-2). In addition, PHEMA was also implanted subcutaneously in experimental animals. The hydrogel samples were explanted after 9 weeks and examined for manifestations of calcification.

Experimental Section

Materials. Dibenzoyl peroxide was obtained from Sigma-Aldrich and twice recrystallized from a mixture of chloroform and methanol. 2-Hydroxyethyl methacrylate (HEMA) stabilized with 300 ppm hydroquinone monomethyl ether (MEHQ), ethyl methacrylate (EMA) stabilized with 15 ppm MEHQ, styrene (St) stabilized with 10−15 ppm 4-*tert*-butyl catechol, and 1-vinyl-2-pyrrolidinone (VP) stabilized with 0.01% NaOH were all supplied by Sigma-Aldrich and purified by vacuum distillation. The chemicals used for preparation of the SBF solutions, including human serum albumin (cat. no. A1653), were used as supplied by Sigma-Aldrich. Water used in all experiments was purified in a Millipore unit.

Synthesis of HEMA-Based Hydrogels. Cylindrical samples of PHEMA and copolymers of HEMA were synthesized to complete conversion (as estimated from FT-NIR spectra by the disappearance of the vinyl peak at 6170 cm^{-1}). The required amount of initiator and monomer(s) were first mixed in standard flasks to give an initiator concentration of 0.05 M. The concentration of EMA, VP, and St was 10 mol % in each HEMA/comonomer mixture. The solutions were then transferred into silicone tubes with an inner diameter of 3 mm and placed in a glass container that can withstand vacuum, flushed with nitrogen gas for 1 h, and gradually degassed to a vacuum between 2.7 and 6.7 hPa. The glass container was then kept in an oven for 20 h at 50 °C, followed by a postcuring treatment for 2 h at 80 °C. The formed glassy polymer rods were removed from the silicon tubes, cut to a 2.5-cm length, and soaked in water to reach the equilibrium swelling at room temperature. Prior to the calcification experiments, all hydrogel samples were hydrated at 37 °C for 2 weeks.

Preparation of SBF Solutions. To prepare SBF-1, we used a formulation[20] that is actually a variant of one of Kokubo's classic formulations.[21,22] SBF-1 contained the following ions (concentrations in mM L^{-1}): sodium (142.0), chlorine (125.0), bicarbonate (27.0), potassium (5.0), magnesium (1.5), calcium (2.5), dibasic phosphate (HPO_4^{2-}) (1.0), and sulfate (0.5). Tris(hydroxymethyl)aminomethane ("Tris" buffer) and hydrochloric acid were used as buffer agents, and the protocol[20] for their addition and for the overall preparation was strictly followed. SBF-2 had the same composition of the inorganic components but additionally contained 0.135 g L^{-1} human serum albumin.

In Vitro Calcification Experiments. Cylindrical hydrogel samples were placed in glass vials containing 20 mL of SBF-1 or SBF-2 and incubated in an oven at 37 ± 0.5 °C for determined periods of time, in duplicate. The time-points for this experiment were at 1, 3, 5, 7, and 9 weeks. After completion, one set of samples was rinsed thoroughly with water, dried, placed in plastic vials, and stored in a desiccator. The duplicate set of samples was kept in water and used for staining experiments.

In Vivo Assessment. Five 11-week old female Wistar rats (weighing between 230 and 260 g) were supplied by the Centre for Breeding, Animal House, University of Queensland. All surgical procedures were performed in accordance to the Australian Code of Practice for the Care and Use of Animals for Scientific Purposes (2003). Under general anesthesia (Halothane), the surgical areas located in the upper back of the animal, above the acromiotrapezius muscle, were shaved, scrubbed with an antiseptic agent (Betadine), and cleaned with 70% ethanol using sterile gauze swabs. The PHEMA specimens were cylinders with a diameter of 3 mm and with a length of 5−7 mm. An approximately 5-mm subcutaneous incision was made with a sterile scalpel for each specimen to be implanted, in total three implants per animal. The dissection of deeper connective tissue was performed using surgical blunt scissors. After the placement of implants, the wounds were closed using Nylon 3-0 sutures.

Nine weeks after surgery, the rats were sacrificed through a humane method in accordance with the Code of Practice mentioned above. Following the death of the animal, an incision of about 10 mm was made at the implantation site and the PHEMA samples were removed with forceps. The hydrogels were immersed in 10% formalin solution and then washed thoroughly in water. Prior to microscopic examination, the hydrogels samples were dehydrated in a graded series of aqueous ethanol.

Staining with Alizarin Red. The presence of calcium in the deposits was examined using a conventional light microscope (Olympus SZH10, Japan), following the staining of samples with alizarin red, a common specific stain for calcium. The staining of the samples that were calcified in SBF-1 and SBF-2 and of the in vivo explants was performed by immersing the samples in a 1% solution of alizarin red in alkaline conditions (0.5% KOH), where they were stored at room temperature for 1 day, followed by washing with water and then keeping them in 0.5% KOH solution until there were no further changes in color. The samples were kept in water for at least 2 weeks prior to observation in the microscope.

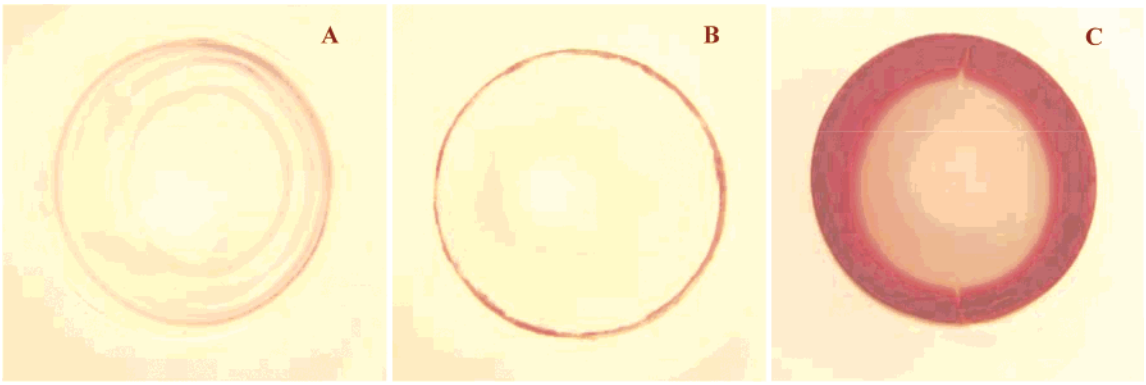

Figure 1. Cross-sectional micrographs of PHEMA specimens stained with alizarin red. Deposition patterns are shown in specimens treated for 9 weeks in SBF-1 (A), SBF-2 (B), and in specimens implanted in animals and removed after 9 weeks (C).

Staining with the von Kossa Method. To obtain some indication on the nature of deposits *inside* the hydrogel samples that were implanted subcutaneously in animals, we employed the von Kossa silver staining method. Although routinely used to detect calcium, this method is in fact specific to the phosphate and carbonate anions. A positive staining proves the presence of any of these anions, rather than calcium; the presence of phosphate, for instance, does not necessarily imply the presence of CaP unless calcium was unambiguously detected in the same sample by a different analytical technique. A recent study[23] demonstrated that von Kossa staining alone is not suitable for the identification and analysis of bone minerals. However, if calcium has already been detected by other means, and based on the generally accepted assumption[24] that in the vertebrates' tissues these anions will almost always appear as calcium salts, a positive von Kossa staining would indeed suggest the presence of CaP phases, very likely of apatite type.

The interior part of the explanted hydrogel samples was cut and separated, then rinsed thoroughly with water, immersed in a 1% solution of silver nitrate, and exposed for 15 min to sunlight. The specimens were then rinsed in water and treated in a 5% solution of sodium thiosulfate for 15 min. Subsequently, the sections were again washed with water and then dehydrated in ethanol, before being examined by conventional microscopy. While the treatment with sodium thiosulfate solution is mandatory in the method in order to remove unreacted silver, it was shown[25] that if carbonate anion is present, the newly formed silver carbonate dissolves in the thiosulfate solution and cannot be properly detected. Therefore, a positive staining is an almost irrefutable proof for the exclusive existence of apatite-type deposits.

Examination by Scanning Electron Microscopy (SEM). The deposits on both in vitro and in vivo hydrogel specimens were examined in an SEM instrument (JEOL 6400F, Japan) at an accelerated electron energy of 5 keV. The samples were dried and coated with platinum.

Examination by X-ray Photoelectron (XPS) and Energy Dispersive X-ray (EDS) Spectroscopies. Semiquantitative analysis of the deposits on both in vitro and in vivo hydrogel specimens was acquired using a Kratos Axis ULTRA XPS instrument incorporating a 165-mm hemispherical electron energy analyzer. The source of X-ray incident radiation was a monochromatic Al Kα (1486.6 eV) at 150 W (15 kV, 10 mA). Survey (wide) scans were taken at an analyzer pass energy of 160 eV and multiplex (narrow) high-resolution scans at 20 eV. Complementary to this analysis, X-ray microelement measurements were performed at an electron energy of 15 keV in a JEOL 6460LA EDS instrument.

Examination by X-ray Diffraction Analysis (XRD). A Bruker AXS D8 Advance XRD instrument was used for this analysis, at an X-ray energy of 1200 W (40 kV, 30 mA). Due to the poor crystallinity and nanometer-scale size of crystals in the CaP deposits, as well as to the difficulty to separate the deposits from the substrate, large amount of material and longer acquisition times were necessary. In this case, a scanning rate of 24.5 s per step with an increment of 0.02° over a 2θ range of 2−70° was used, which required about 24 h to obtain a relatively well-resolved spectrum.

Results and Discussion

Calcification of Hydrogels in SBF. If, as expected, albumin is implicated in the calcification process, its behavior at the interface with hydrogels has a crucial importance. At least two concurrent mechanisms through which albumin can become involved in the process may be envisaged: (a) a layer of albumin adsorbed on the surface of polymer can mask the existing functional groups, such affecting or even precluding, their contribution to the process, and (b) calcium ions can chelate to albumin before binding electrostatically to phosphate anions. If the adsorption of albumin at the interface is the only event to occur, the subsequent CaP deposit formation will be restricted to a peripheral zone on the surface of hydrogel specimens. However, if albumin can also penetrate the hydrogel network, the deposition pattern will be quite different, extending into the interior of specimens. The ability of albumin to penetrate a polymer network is primarily dictated by its molecular dimensions. The data available on the shape and size of albumin molecule have not been very consistent. Various reports referred either to a globular shape with a diameter of 5.44 nm,[26] or an ellipsoidal shape with axes of 4.5 and 14.4 nm, respectively,[27] or to a solid equilateral triangle with sides of 8 nm and depth of 3 nm.[28] Despite such variability, the existing studies unambiguously agree that albumin is only adsorbed on the surface of PHEMA (and other HEMA-based hydrogels) and cannot penetrate the polymer network.[29−35] We expect therefore that the CaP deposits resulting from the calcification experiment carried out in SBF-2 will be formed exclusively on the surface.

This evidence was indeed provided by the alizarin red staining experiment, as shown in Figure 1B for PHEMA. There is no staining caused by the calcium presence inside the hydrogel cylinder, and the deposits are concentrated exclusively along the peripheral region. By contrast, in SBF-1, which does not contain albumin, the CaP deposits were found both on the surface and advancing toward the interior regions in consecutive fronts of diminishing intensity, as seen in Figure 1A. Although the formation of CaP deposits inside the hydrogels in organic-free media has been investigated in our previous reports,[9,36] this is the first time when the occurrence of advancing concentric fronts of deposited CaP was noticed. At this stage we can only speculate that this may be a manifestation of the Liesegang phenomenon,[37] which occurs in diffusion−reaction systems and has been recently demonstrated in the case of precipitation of CaP in silica gel cylinders as consecutive deposition rings,[38]

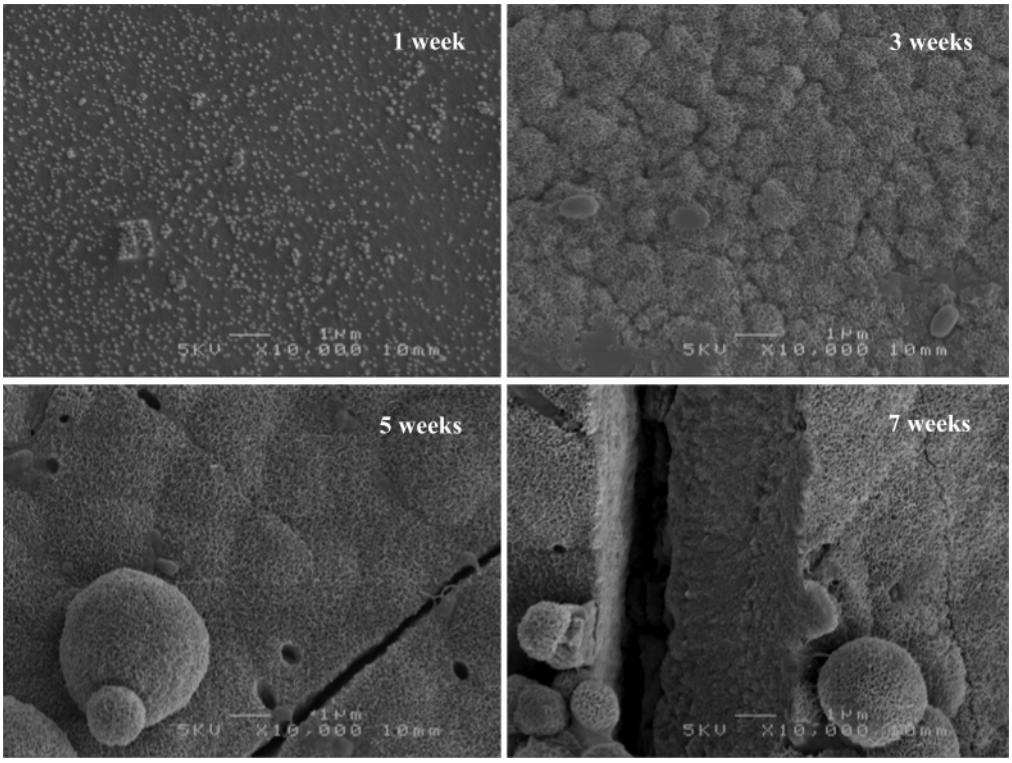

Figure 2. SEM images of PHEMA hydrogels after incubation in SBF-2 for various durations. Scale bar: 1 μm.

when examined longitudinally. However, in the present study the features were noticed transversally (as in Figure 1A); it can also be argued that the system underlying the precipitation process in our experiment may not be a proper diffusion−reaction system.

The patterns of deposition in SBF-2 showed no significant difference between PHEMA and the copolymers. This was previously shown[36] to be also the case in SBF-1. Therefore, the results of this study are exemplified on PHEMA only.

The SEM images presented in Figure 2 show the morphology of the CaP deposits formed during incubation in SBF-2. As expected, upon increasing the calcification time, the size of the deposited structures increased gradually until they eventually reached confluence to form a CaP layer with a thickness of about 4 μm. The morphology of the CaP deposits seems to be independent of the chemical structure of hydrogels, as there were no differences between the deposits formed on the various polymer formulations.

The differences between the morphology of the deposits generated in SBF-1 and those generated in SBF-2, as shown in Figure 3, are rather difficult to fathom. Large spherical agglomerates seem to be in a greater number in the deposits formed in SBF-2.

The microanalysis of the deposits by XPS revealed more subtle differences induced by the presence of albumin. The survey scan spectra shown in Figure 4 demonstrate that the CaP deposits generated in SBF-2 contain nitrogen, but lack magnesium, albeit the EDS analysis detected traces of this element. The absence of Mg, or its presence in minute amounts, suggests that the CaP deposits are unlikely to be apatites of whitlockite type. However, whitlockite appears to be the main constituent in the CaP deposits formed during incubation of HEMA-based hydrogels in SBF-1.

Additionally, as the Ca/P molar ratios for the samples calcified in SBF-2 for at least 5 weeks lie in the range of 1.2−2.2 (see Table 1), the CaP deposits were more likely to consist of mainly hydroxyapatite deficient in calcium and hydroxyl ions, also known as "precipitated hydroxyapatite". The presence of N in the SBF-2-generated deposits was believed to originate from the albumin, yet N originating from "Tris" buffer (added in the preparation of the SBFs) was detected in the early stage of calcification, particularly in the samples treated in SBF-1.

Table 1. XPS Data of the CaP Deposits Formed on the Surface of Hydrogels upon Incubation in SBF-2 for Various Durations

	mass concentration (%)					molar ratio
sample[a]	C 1s	O 1s	Ca 2p	P 2p	N 1s	Ca/P
A5	51.57	29.54	8.67	5.35	4.52	1.25
A7	38.54	35.85	13.85	7.54	3.37	1.42
A9	34.69	31.29	19.08	9.17	5.27	1.61
B5	35.49	37.45	15.05	7.86	3.55	1.48
B7	41.17	35.38	11.46	5.61	5.54	1.58
B9	31.98	37.17	17.44	8.29	4.54	1.63
C5	47.50	29.92	9.08	5.58	6.01	1.36
C7	43.57	30.08	12.53	7.24	5.34	1.34
C9	37.04	35.64	12.32	6.80	5.89	1.40
D5	39.94	37.22	12.50	5.70	3.28	1.69
D7	41.03	39.93	11.19	6.63	5.44	1.30
D9	42.62	34.86	11.04	4.03	6.93	2.12

[a] A, PHEMA; B, P(HEMA-*co*-EMA); C, P(HEMA-*co*-VP); D, P(HEMA-*co*-St); nos. 5, 7, and 9 denote the duration in weeks.

This result was in accordance with the XPS data presented in Figure 5, where the presence of N in the CaP deposits formed in SBF-2 was persistent and its amount increased over that for SBF-1. On the contrary, the presence of N in the deposits generated in SBF-1 decreased in time, and it was no longer detectable after 5 weeks, when the entire surface of the hydrogel became covered by CaP deposits. This trend suggests that albumin was involved in the mechanism of CaP deposition, probably by chelation of calcium ions, which may lead to nucleation centers from which CaP nodules can grow and eventually form precipitates. It also suggests that "Tris" buffer was not involved in the calcification process.

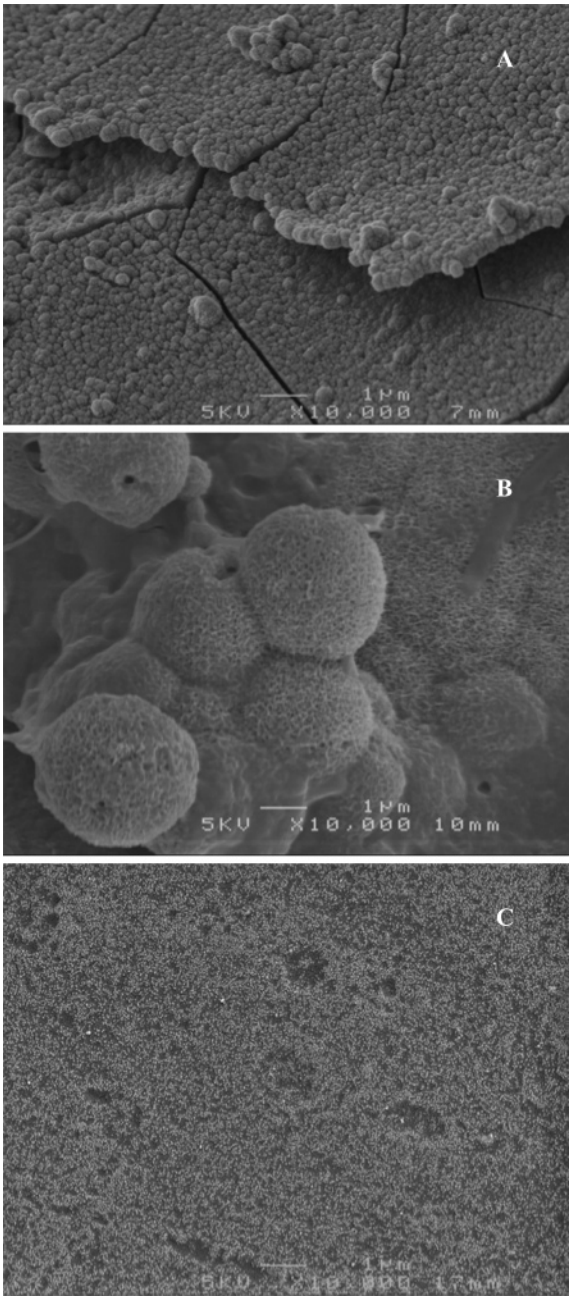

Figure 3. SEM images of PHEMA specimens treated for 9 weeks in SBF-1 (A), SBF-2 (B), and in specimens implanted in animals and removed after 9 weeks (C). Scale bar: 1 μm.

The high-resolution C 1s XPS spectrum of the deposits generated in SBF-2 show the presence of 6 peaks, compared with only 3 peaks in the C 1s spectrum of those generated in SBF-1, as seen in Figure 6.

As summarized in Table 2, the major peaks have been associated, respectively, with aliphatic/albumin carbon, C−C/C−H (284.90 eV), apatite carbonate carbon, C−O (286.28 eV), and the albumin amide carbon, N−C═O (288.29 eV). The remaining small peaks correspond, respectively, to the C−N, C−O, and HO−C═O groups in albumin. The O 1s XPS spectra (also shown in Figure 6 and summarized in Table 2) reveal that due to the additional oxygen from albumin (C−O and C═O) the intensity of the carbonate peak at 532.49 eV increased in the deposits generated in SBF-2, producing a more asymmetric peak when compared with the O 1s peak of the deposits generated in SBF-1. The peak at 531.10 eV is due to the three equivalent oxygen atoms linked to the phosphorus atom. The peak which appears at 533.31 eV corresponds to the oxygen atom which is linked to both phosphorus and hydrogen atoms. The last peak appears at the highest binding energy because O in P−O−H is less charged as compared to O in C−O and P−O.

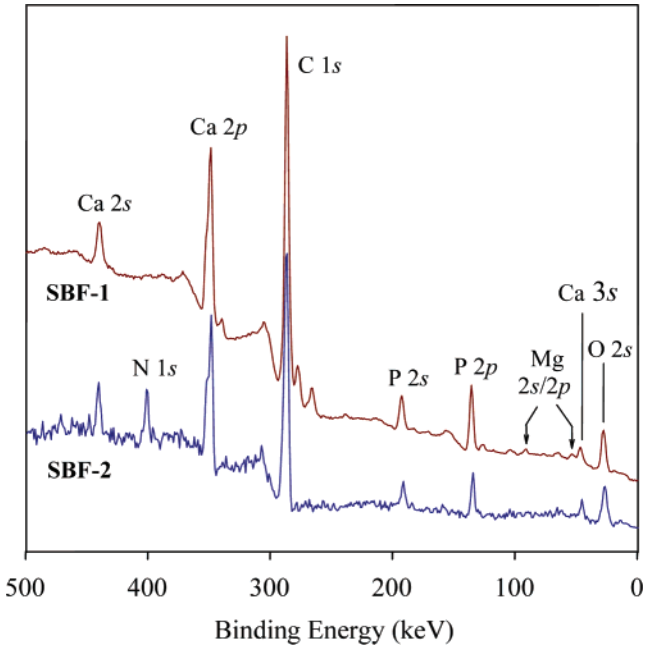

Figure 4. XPS spectra (survey scans) of CaP deposits formed on PHEMA after incubation for 9 weeks in each SBF.

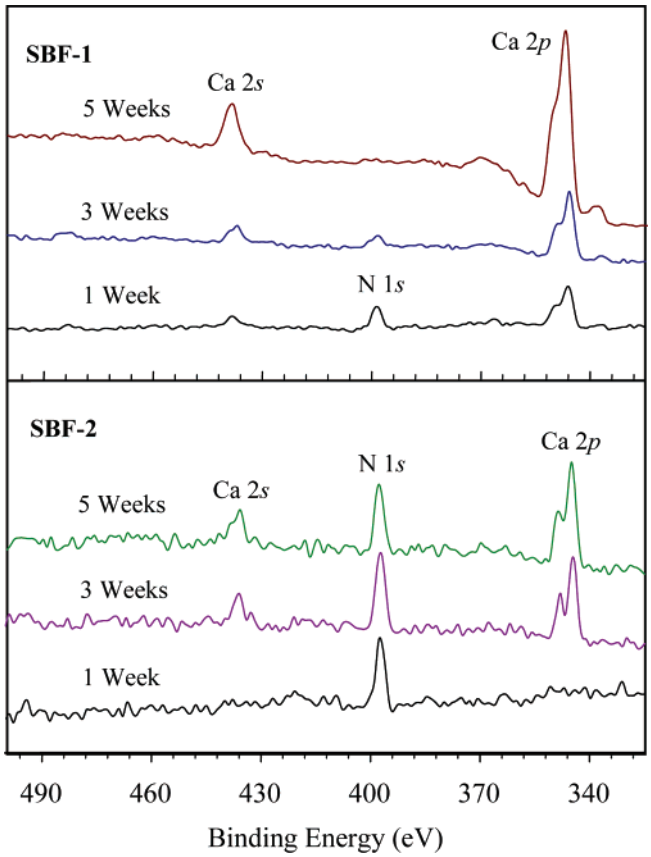

Figure 5. Effect of the duration of incubation in each SBF on the XPS spectra (survey scans) for N 1s of CaP deposits formed on PHEMA.

Furthermore, the high-resolution N 1s XPS spectrum of the deposits generated in SBF-2 (Figure 7) confirmed the involvement of albumin in their formation. As assigned in Table 2, the

Table 2. Peak Assignments for C 1s, O 1s, and N 1s XPS Spectra of the PHEMA Substrate and of the Deposits Formed after Incubation in SBF-1 and SBF-2 for 9 Weeks

treatment	C 1s peak position (eV)	C type	O 1s peak position (eV)	O type	N 1s peak position (eV)	N type
water[a]	285.02	C−H	532.28	O=C		
	285.65	C−C	533.00	O−H		
	286.57	C−OH	533.84	O−C		
	286.98	C−O				
	289.12	C=O				
SBF-1	285.03	C−H[b]	531.15	O−P		
	286.25	C−O[c]	532.11	O−C		
	288.90	C=O[b]	533.36	H−O−P		
SBF-2	284.90	C−C/C−H	531.10	O−P	399.96	N−H
	285.70	C−N	532.49	O−C	401.50	N−C
	286.28	C−O[c]	533.31	H−O−P		
	287.50	C−O[d]				
	288.29	C=O				
	289.40	HO−C=O				

[a] PHEMA. [b] Unknown contaminants. [c] In carbonate. [d] In albumin.

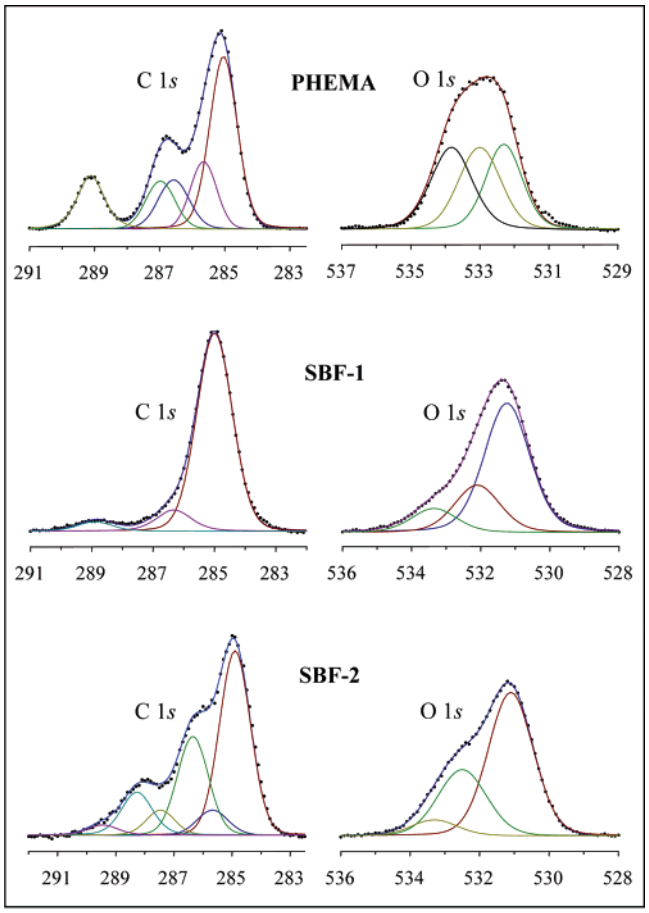

Figure 6. High-resolution C 1s and O 1s XPS spectra of CaP deposits formed on PHEMA after incubation for 9 weeks in each SBF.

peaks which appear at 399.96 and 401.50 eV are associated with the N−H and N−C moieties, respectively.

In Vivo Calcification. The micrograph in Figure 1C shows the calcification pattern of PHEMA that occurred over 9 weeks following their subcutaneous implantation in rats. The deposits (about 0.4 mm in thickness) which covered the whole surface of the PHEMA hydrogels contained calcium in abundance, most probably in the form of CaP phases, as reflected by the intense orange-red color from the deposits stained with alizarin red.

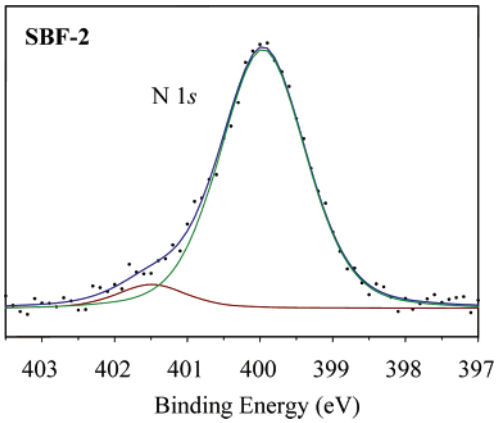

Figure 7. High-resolution N 1s XPS spectrum of CaP deposits formed on PHEMA after incubation for 9 weeks in SBF-2.

Although very weak in intensity, the staining occurring inside the hydrogel was an indication that some calcium deposits were advancing toward the interior zone. However, the latter deposits are likely Ca−biomacromolecule complexes rather than deposited CaP phases, which is supported indeed by the lack of staining with the von Kossa method, such confirming that the calcium deposits inside the hydrogels are not apatitic. Figure 1C also indicates that the formation of CaP deposits is limited to the surface of the hydrogels, and this may be due to a process which is mainly mediated by the adsorbed proteins. Indeed, an early hypothesis assumed that the process of calcification in a biological environment was initiated by nucleation of CaP in the adsorbed layer of proteins.[39,40] The thickness of the deposited layer is much greater than that of the layer generated in SBF-2 over the same period of time (Figure 1B). In comparison with the morphology of the deposits formed in SBF-2 (Figure 3B), the morphology of the in vivo CaP deposits (Figure 3C) is also different, being composed of very fine spherical agglomerates.

The XRD patterns acquired for the deposits are presented in Figure 8. All peaks are broad, indicating that the deposits are composed of nanocrystalline or amorphous precipitates. Comparing with the reference XRD data for brushite and hydroxyapatite, the patterns of the both deposits closely match those of hydroxyapatite reflections. This certainly suggests that the types of the deposits, either arising from SBF-2 or in vivo, contain similar CaP phases, composed mainly of "precipitated hydroxyapatite" and hydroxyapatite, accompanied by small quantities of calcium carbonate phase and brushite. Additionally, the

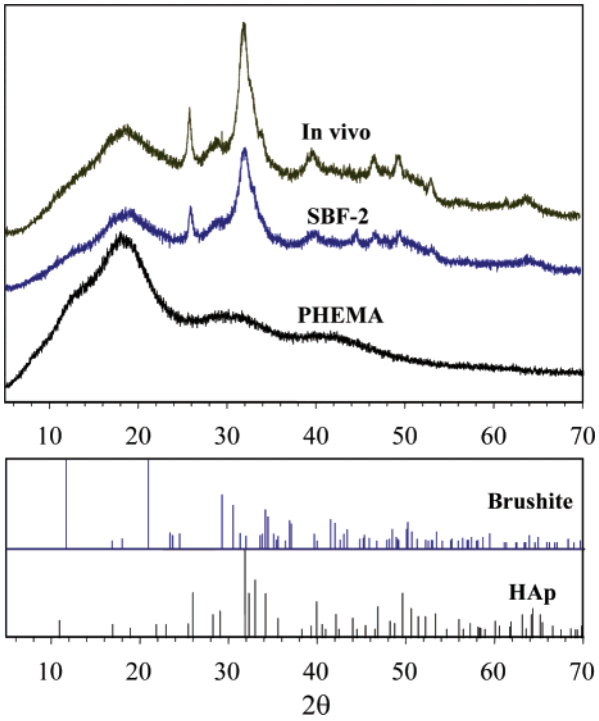

Figure 8. XRD patterns of CaP deposits formed on PHEMA after 9 weeks in vivo and in SBF-2. The control was treated in water.

Table 3. XRD Reflections of the CaP Phases in Deposits Formed on PHEMA in SBF-2 and in Vivo

2θ	reflection	CaP phase[a]	treatment
25.90	002	HAp	in vivo, SBF-2
29.29	11-2	brushite	in vivo, SBF-2
32.22	112	HAp	in vivo, SBF-2
34.09	202	CHAp/HAp	in vivo
39.26	212	CHAp	in vivo, SBF-2
43.91	113	HAp	in vivo
44.85	211	CHAp	SBF-2
46.42	401	HAp	in vivo, SBF-2
49.26	013	brushite	in vivo, SBF-2
53.09	310	brushite	in vivo, SBF-2
61.75	214	HAp	in vivo
64.02	304	HAp/brushite	in vivo, SBF-2

[a] Abbreviations: HAp, hydroxyapatite; CHAp, carbonated hydroxyapatite.

two patterns also appear to be similar to the XRD patterns of dentine and bone.[41] The complete assignments for all peaks, based on the existing literature[42−44] and corresponding to hydroxyapatite, carbonated hydroxyapatite, and brushite reflections, are tabulated in Table 3.

The FTIR spectra (Figure 9) of the deposits and other materials for comparison indicate much similarity between the deposits formed in vivo (Figure 9C) and in SBF-2 (Figure 9B). Although the bands characteristic to the PHEMA substrate (Figure 9A) are interfering, it can be seen that the spectra of the deposits resemble the spectra of bone (Figure 9E) and synthetic carbonated hydroxyapatite (Figure 9F), rather than that of calcium carbonate (Figure 9D). Calcium carbonate phases are commonly found as minor constituents of biological apatites. Their infrared vibrational bands were reported to be similar to those of synthetic carbonated apatites but different from those of simple carbonates, such as $CaCO_3$, Na_2CO_3, and $MgCO_3$.[41] This difference can be seen in Figure 9, where the infrared spectrum for carbonate ions in the region of 1350−1650 cm^{-1}

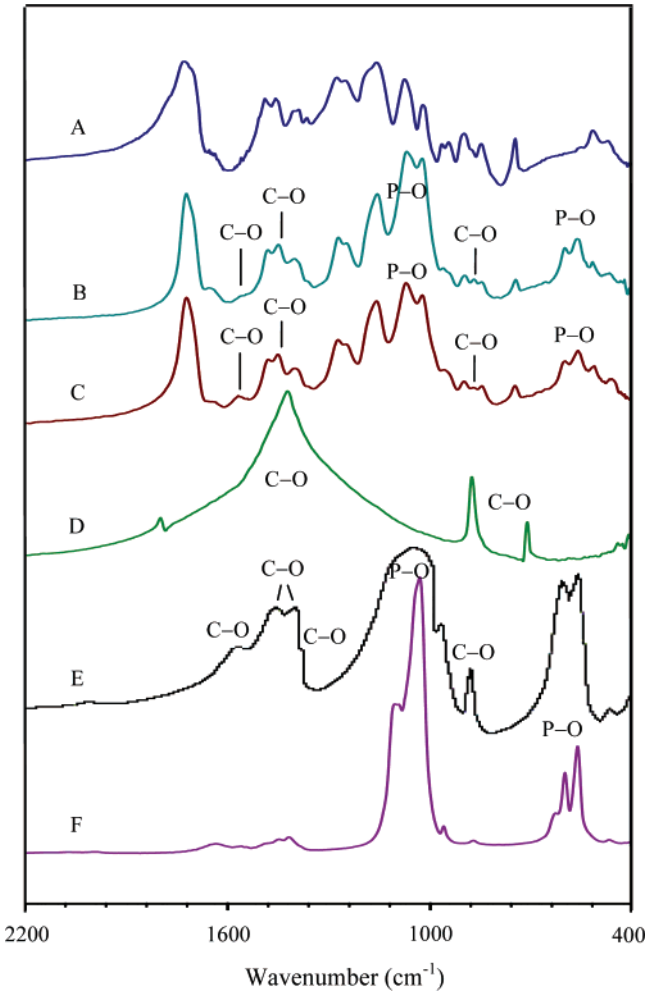

Figure 9. FTIR spectra of (A) PHEMA, (B) CaP deposits after 9 weeks in SBF-2, (C) in vivo CaP deposits (specimens explanted at 9 weeks), (D) $CaCO_3$, (E) human bone (adapted from ref 41), and (F) synthetic carbonated hydroxyapatite.

shows four bands in carbonated hydroxyapatite, while only one band is present in the spectrum of $CaCO_3$.

Conclusions

Although it is expected that the mechanism of calcification in a biological environment is more complex than in simulated body fluid formulations containing albumin, the latter can serve as a reasonable model for in vivo calcification of synthetic hydrogels. This is mainly because (a) the type of CaP phases and the crystallinity of the deposits formed in both systems appear to be similar and (b) both systems involve the adsorption of proteins onto the surface of hydrogels, which then become involved in the formation of CaP deposits.

The only significant differences between the in vitro and the in vivo results of this study can be seen in the morphology and density of the CaP deposits. Those formed in SBF-2 consisted of much larger globular structures which were less packed, and the deposited layer was much thinner as compared to the layer formed in vivo.

Acknowledgment. This study was supported by a Grant from the Australian Research Council (DP0208223). Support from the University of Queensland for a postgraduate research scholarship to one of the authors (Z.) is also acknowledged. The authors thank Dr. Barry Wood, John Nailon, Anya Yago,

and Kim Sewell for assistance in using the XPS, SEM, XRD, and EDS instrumentations, Dr. Michelle Newman and Craig Dickfos for supervising the animal experiments, and Shuko Suzuki for kindly providing a sample of synthetic carbonated hydroxyapatite.

References and Notes

(1) Ruben, M.; Tripathi, R. C.; Winder, A. F. *Br. J. Ophthalmol.* **1975**, *59*, 141−148.
(2) Abbott, J. M.; Bowers, R. W. J.; Franklin, V. J.; Tighe, B. J. *J. Br. Contact Lens Assoc.* **1991**, *14*, 21−28.
(3) Tighe, B.; Franklin, V. In *The Eye in Contact Lens Wear*, 2nd ed.; Larke, J. R., Ed.; Butterworth-Heinemann: Boston, 1997; pp 49−100.
(4) Werner, L.; Apple, D. J.; Kaskaloglu, M.; Pandey, S. K. *J. Cataract Refractive Surg.* **2001**, *27*, 1485−1492.
(5) Dorey, M. V.; Brownstein, S.; Hill, V. E.; Mathew, B.; Botton, G.; Kertes, P. J.; El-Defrawy, S. *Am. J. Ophthalmol.* **2003**, *135*, 591−598.
(6) Chirila, T. V.; Morrison, D. A.; Hicks, C. R.; Gridneva, Z.; Barry, C. J.; Vijayasekaran, S. *Cornea* **2004**, *23*, 620−629.
(7) Vijayasekaran, S.; Chirila, T. V.; Robertson, T. A.; Lou, X.; Fitton, J. H.; Hicks, C. R.; Constable, I. J. *J. Biomater. Sci., Polym. Ed.* **2000**, *11*, 599−615.
(8) Chirila, T. V.; Gridneva, Z.; Morrison, D. A.; Barry, C. J.; Hicks, C. R.; Hill, D. J. T.; Whittaker, A. K.; Zainuddin *J. Mater. Sci.* **2004**, *39*, 1861−1864.
(9) Zainuddin; Chirila, T. V.; Hill, D. J. T.; Whittaker, A. K. *J. Mol. Struct.* **2005**, *739*, 199−206.
(10) Chirila, T. V.; Morrison, D. A.; Gridneva, Z.; Garcia, A. J. A.; Platten, S. T.; Griffin, B. J.; Zainuddin; Whittaker, A. K.; Hill, D. J. T. *J. Mater. Sci.* **2005**, *40*, 4987−4990.
(11) Chirila, T. V.; Morrison, D. A.; Gridneva, Z.; Meyrick, D.; Hicks, C. R.; Webb, J. M. *Contact Lens Anterior Eye* **2005**, *28*, 21−28.
(12) Combes, C.; Rey, C. *Biomaterials* **2002**, *23*, 2817−2823.
(13) Held, I. R.; Freeman, S. *J. Appl. Physiol.* **1964**, *19*, 292−296.
(14) Pedersen, K. O. *Scand. J. Clin. Lab. Invest.* **1971**, *28*, 459−469.
(15) Besarab, A.; Deguzman, A.; Swanson, J. W. *J. Clin. Pathol.* **1981**, *34*, 1361−1367.
(16) Campbell, A. A.; Ebrahimpour, A.; Perez, L.; Smesko, S. A.; Nancollas, G. H. *Calcif. Tissue Int.* **1989**, *45*, 122−128.
(17) Ebrahimpour, A.; Perez, L.; Nancollas, G. H. *Langmuir* **1991**, *7*, 577−583.
(18) Combes, C.; Rey, C.; Freche, M. *J. Mater. Sci.: Mater. Med.* **1999**, *10*, 153−160.
(19) Serro, A. P.; Fernandes, A. C.; Saramago, B.; Fernandes, M. H. V. *J. Biomed. Mater. Res.* **2002**, *61*, 99−108.
(20) Tas, A. C. *Biomaterials* **2000**, *21*, 1429−1438.
(21) Ohtsuki, C.; Kokubo, T.; Yamamuro, T. *J. Non-Cryst. Solids* **1992**, *143*, 84−92.
(22) Li, P.; Ohtsuki, C.; Kokubo, T.; Nakanishi, K.; Soga, N.; Nakamura, T.; Yamamuro, T. *J. Am. Ceram. Soc.* **1992**, *75*, 2094−2097.
(23) Bonewald, L. F.; Harris, S. E.; Rosser, J.; Dallas, M. R.; Dallas, S. L.; Camacho, N. P.; Boyan, B.; Boskey, A. *Calcif. Tissue Int.* **2003**, *72*, 537−547.
(24) Prento, P. In *Theory and Strategy in Histochemistry*; Lyon, H., Ed.; Springer: Berlin, 1991; p 226.
(25) Meloan, S. N.; Puchtler, H. *J. Histotechnol.* **1985**, *8*, 11−13.
(26) Rodbard, D.; Chrambach, A. *Anal. Biochem.* **1971**, *40*, 95−134.
(27) Colton, C. K.; Smith, K. A.; Merrill, E. W.; Farrell, P. C. *J. Biomed. Mater. Res.* **1971**, *5*, 459−488.
(28) He, X. M.; Carter, D. C. *Nature* **1992**, *358*, 209−215.
(29) Refojo, M. F.; Leong, F.-L. *J. Polym. Sci., Polym. Symp.* **1979**, *66*, 227−237.
(30) Castillo, E. J.; Koenig, J. L.; Anderson, J. M.; Lo, J. *Biomaterials* **1984**, *5*, 319−325.
(31) Ishihara, K.; Nomura, H.; Mihara, T.; Kurita, K.; Iwasaki, Y.; Nakabayashi, N. *J. Biomed. Mater. Res.* **1998**, *39*, 323−330.
(32) Garrett, Q.; Milthorpe, B. K. *Invest. Ophthalmol. Visual Sci.* **1996**, *37*, 2594−2602.
(33) Garrett, Q.; Chatelier, R. C.; Griesser, H. J.; Milthorpe, B. K. *Biomaterials* **1998**, *19*, 2175−2186.
(34) Garrett, Q.; Griesser, H. J.; Milthorpe, B. K.; Garrett, R. W. *Biomaterials* **1999**, *20*, 1345−1356.
(35) Garrett, Q.; Laycock, B.; Garrett, R. W. *Invest. Ophthalmol. Visual Sci.* **2000**, *41*, 1687−1695.
(36) Zainuddin; Hill, D. J. T.; Whittaker, A. K.; Chirila, T. V. *J. Mater. Sci.: Mater. Med.*, in press.
(37) Henisch, H. K. *Crystals in Gels and Liesegang Rings*; Cambridge University Press: Cambridge, 1988.
(38) George, J.; Varghese, G. *J. Mater. Sci.* **2005**, *40*, 5557−5559.
(39) Rosanova, I. B.; Mishchenko, B. P.; Zaitsev, V. V.; Vasin, S. L.; Sevastianov, V. I. *J. Biomed. Mater. Res.* **1991**, *25*, 277−280.
(40) Vasin, S. L.; Rosanova, I. B.; Sevastianov, V. I. *J. Biomed. Mater. Res.* **1998**, *39*, 491−497.
(41) LeGeros, R. Z. In *Hydroxyapatite and Related Materials*; Brown, P. W., Constantz, B., Eds.; CRC: Boca Raton, FL, 1994; pp 3−28.
(42) Brophy, G. P.; Nash, J. T. *Am. Mineral.* **1968**, *53*, 445−454.
(43) Curry, N. A.; Jones, D. W. *J. Chem. Soc.* **1971**, 3725−3729.
(44) Hughes, J. M.; Cameron, M.; Crowley, K. D. *Am. Mineral.* **1989**, *74*, 870−876.

BM060075G